

Figure 1: Global structure of the ADI system

The voltage equations may be expressed by structural diagram as on figure 2.

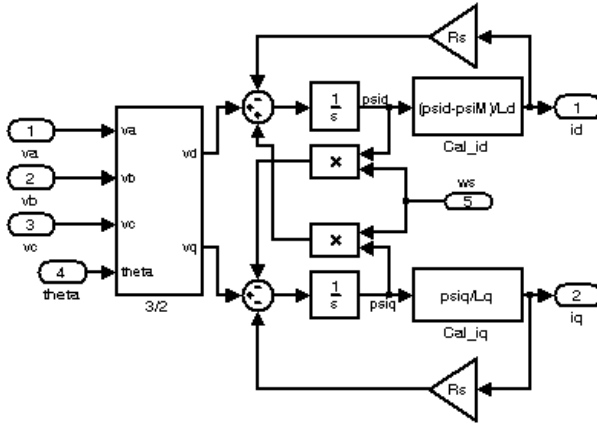


Figure 2: structural diagram of a linear IPMSM

### II.1.2. Taking into account of the magnetic saturation

As seen on the figure 1, the unique source of non-linearity is the link between the flux and the currents. The phenomenon is complex and lots of papers try to give an analytic or semi analytic expression [7-14].

Beyond that, IPMSM has high level of coupling between the two axes, so the determination of  $\psi_d$  requires to compute the contribution of  $i_d$  but also of  $i_q$ . The coupling between d and q axis become unavoidable.

Nevertheless, the projection of space vectors on a frame linked to the rotor remains possible (purely geometric transformation) [13].

The dynamic modelling of the cross saturation in permanent magnet machines remains difficult. Some publications deal with this subject [12, 13, 15] and we propose an original method.

The proposed solution is split in two parts:

- Determination of  $\psi_d$  and  $\psi_q$  as a function of  $i_d$  and  $i_q$  by an off line FE method (FLUX 2D). This method is exposed in [16].
- Linearisation and inversion of the proposed model.

Although, a comprehensive description is not the subject of this paper, the presented results use this approach. This model is detailed in [17].

## II.2. TORQUE REFERENCE

Torque reference depends on the operating mode:

- Starter mode: high positive reference, equivalent to the maximum machine torque;
- Boost (i.e. motor) mode: same as starter mode, or power regulation between thermal and electric motor;
- Regenerative braking: high negative reference, equivalent to the maximum negative machine torque;
- Generator mode: DC voltage regulation.

## II.3. OPTIMAL CONTROL

Several optimal current tables are used for the different operating modes. Each table gives current references  $i_d^*$  and  $i_q^*$  as a function of the torque reference and the speed measurement. The optimal control strategies have been previously described in [16, 18].

## II.4. CURRENT REGULATION

The current regulation gives the voltage references used to drive each half-bridge of the inverter. Several regulation may be used:

- (P, PI...) on each phase;
- direct and quadrature axis current regulation;
- Direct and quadrature axis current regulation (PI), with back-EMF compensation is preferably used as recommended in [19].

These different types of regulation have been tested and the presented results use the third approach.

## II.5. INVERTER

All PWM strategies can be simulated: natural sampling, space vector modulation, delta-sigma, ad. In this study, a natural sampling (Sinusoidal PWM), simple but well-known, is used. For more details about strategies, please refer to [20,21].

Each phase voltage can be deduced from the half-bridge voltage reference and DC voltage value. Other inverter models are developed [21], which take into account of resistance, capacitance and inductance in the inverter components and give its losses.

## II.6. BATTERY (DC BUS)

Classically, battery is first modelled by a voltage source associated with an internal resistance. The DC bus is modelled by a stray inductance and a DC-link capacitor.

More precise dynamic models are under development [22] and can be used instead of the simple model.

## II.7. MECHANICAL LOAD

The mechanical load is constituted by the ICE and so, is very difficult to model.

The mechanical load depends on the operating mode (starter, booster, generator). In motor mode, the load is inertial and takes into account of friction damping. In generator mode, the machine is driven at variable speeds between 0 and 6000 rpm. Speed acyclisms may be added.

A precise model is now developed [23]. This model requires lots of data concerning the thermal engine with all its components. In this study, we will keep the previous model.

## III. TORQUE STEP RESPONSE

In this part, we will show the dynamic response to a torque step test at constant speed. This test is done in generator

mode, electric power is absorbed by an active load which regulates the DC voltage to 42V.

### III.1. EXPERIMENT

#### III.1.1. Test bench

Figure 3 shows the global test bench (LEC). The load machine is driven up to 10000 rpm and 100 Nm (at low speed) and the bench is specially adapted to ISG (and SG).

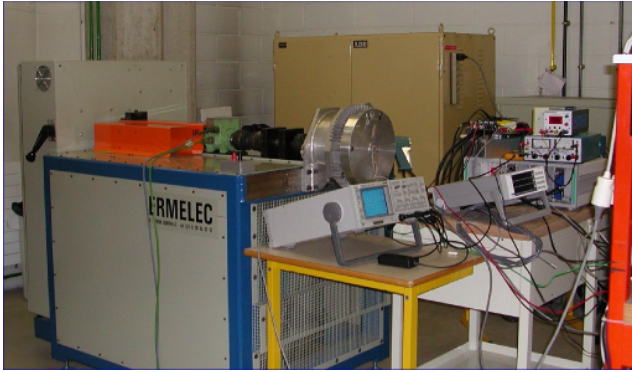


Figure 3: Test bench

Figure 4 shows the detail of the inverter developed by the LEC, (200 A @ 10 kHz).

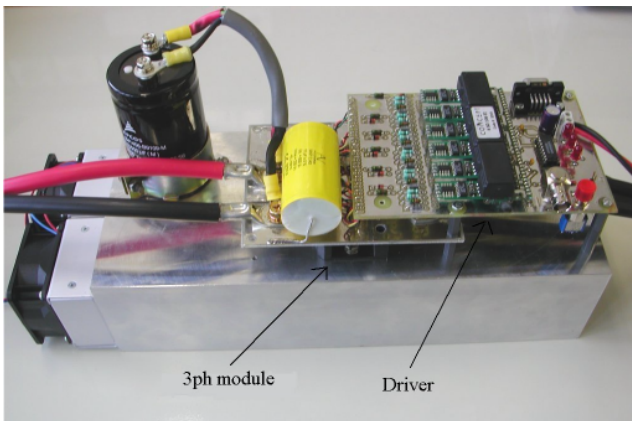


Figure 4: Inverter (LEC)

Figure 5 shows more precisely the ISG. The integrated topology is immediately pointed out. We can see a specific developed resolver for the rotor position acquisition.

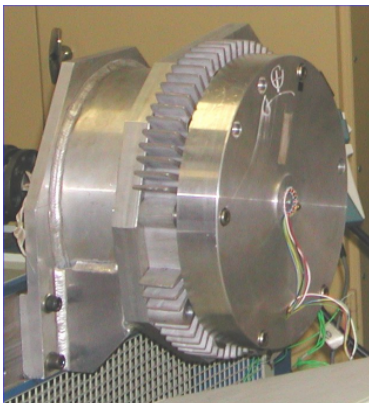


Figure 5: ISG (Valeo)

All the acquisitions (rotor position, phases currents, temperature, ad.) and control are done by a DSpace card (DS1103).

### III.2. SIMULATION AND RESULTS

The simulation takes into account of all real components:

- Machine: saturation and losses (copper, iron, mechanical);
- Inverter: SPWM (chopping effects taken into account);
- DC load: active load
- DC line filter (LC)
- Speed is constant;
- Torque reference consists of a step from -5 Nm to -20 Nm (generator).

Next figures show the evolution of torques,  $i_d$  and  $i_q$  (reference, simulation and measures).

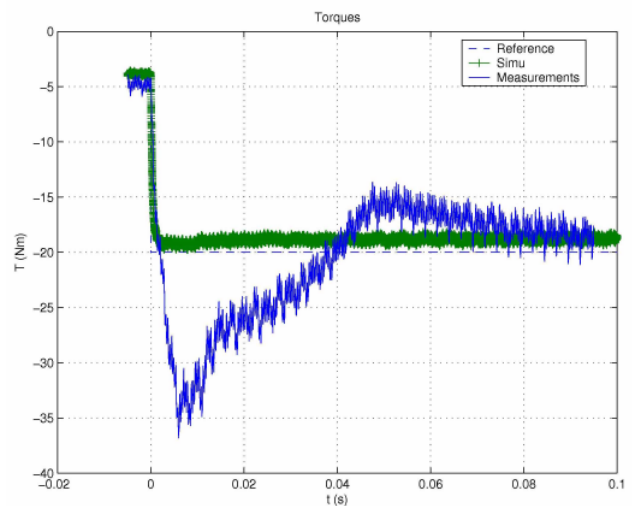


Figure 6: torques (reference, simulation and measures)

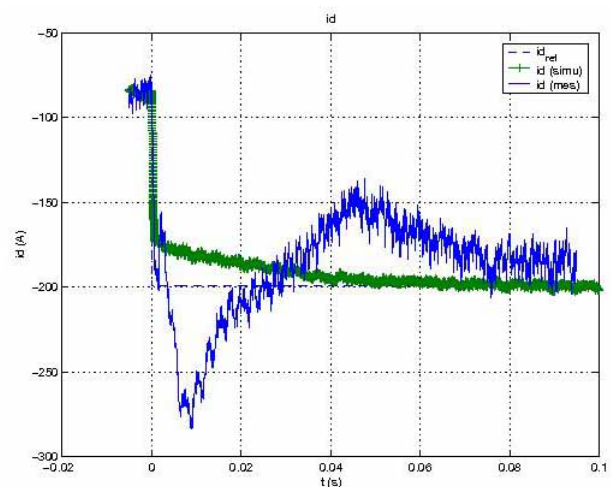


Figure 7: Comparison of  $i_d$  reference, simulation and measures

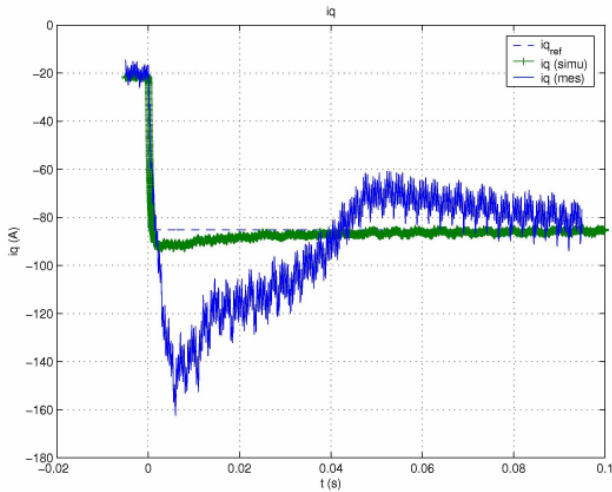


Figure 8: Comparison of  $i_q$  reference, simulation, and measures

Observations:

- At 3000 rpm, the main current is the d-axis current in order to obtain the optimal flux-weakening;
- Current regulators are efficient, d and q currents follow strictly and quickly the current reference from the optimal control tables.
- The power step required (4,5 kW) is available in less than 60 ms.

#### IV. ICE STARTING SEQUENCE SIMULATION

In this part, a complete ICE starting sequence, followed by the beginning of a DC voltage regulation, is simulated. All the components of the real system are taken into account.

Figures 9 and 10 show some results of this simulation: speed, torques (reference, machine and load), d-q currents, phases currents, and finally DC bus currents and voltage.

Some remarks can be done:

- The optimal control gives the desired results: it tries to follow the torque reference (150 Nm) and develops its maximum torque (140 Nm) until 120 ms about. Then, the electric power increases and the DC voltage supply drops. Thus, currents and torque are falling too, but currents stay always under control. Without taking into account of the battery voltage (global system approach) during optimal laws calculation, this phenomenon would have been neglected and the inverter would have lost currents control (See figures 9, 10 and 11a);
- Direct and quadrature currents follow the references given by the optimal control. Current

regulators are efficient, fast and  $i_d$  and  $i_q$  currents are decoupled (See figure 10);

- In starter mode, DC voltage drops when the machine power increases. In generator mode, voltage is regulated around 42V. A quite simple regulation (PI) obtains good results (See figure 11a).
- It is interesting to see the influence of DC link capacitor: battery current is quite smooth whereas DC bus current is perturbed by the PWM (See figure 11b). This approach can be used to design the DC link capacitor considering all the system.

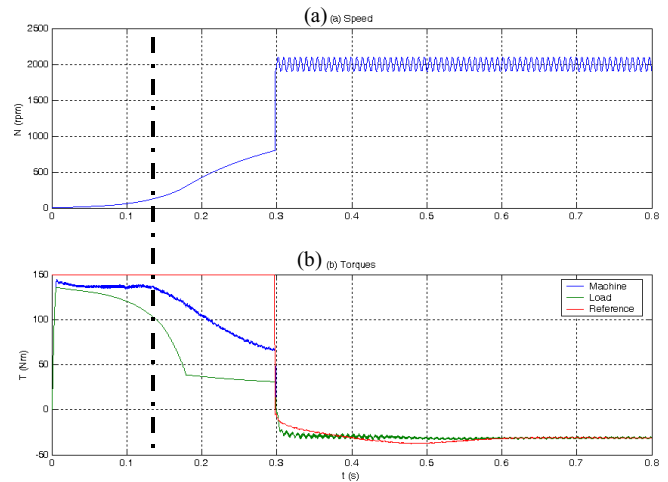


Figure 9: Speed and torques

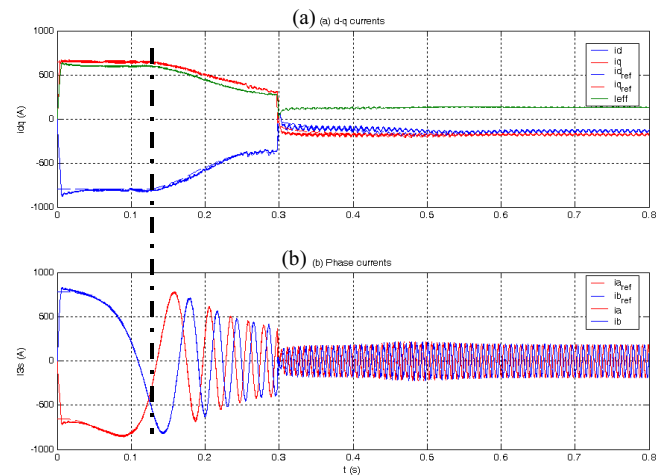


Figure 10: d-q and phases currents

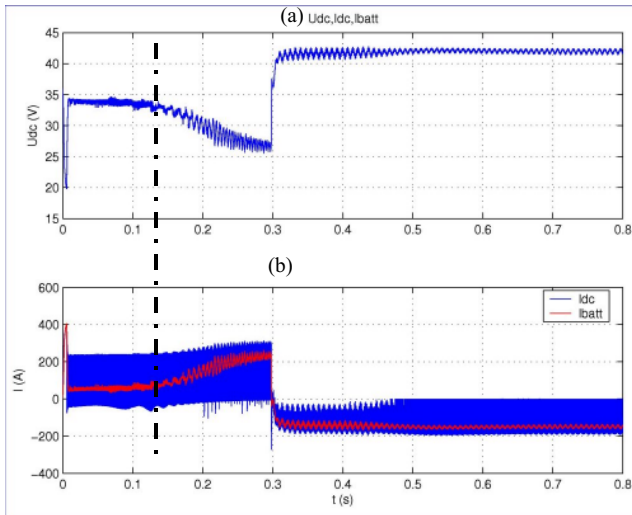


Figure 11: DC bus voltages and currents

## V. CONCLUSION

A dynamic model of an ISG system has been presented (Electric machine, power electronics, battery, control). Experimental results show the good accuracy of the model, even for difficult modeling phenomena (cross saturation, current control, DC bus).

A whole ICE starting sequence has been simulated. All presented results show that a well designed IPMSM may have interesting flux weakening performances and so is a challenger to the induction machine in ISG applications.

## VI. REFERENCES

- [1] B.J. Chalmers, L. Musaba, and D.F. Gosden. Variable-frequency synchronous motor drives for electrical vehicles. *IEEE Trans. Ind. Appl.*, 32(4):896-903, Jul./Aug. 1996.
- [2] E.C. Lovelace, T.M. Jahns, J.L. Kirtley, and J.H. Lang. An interior PM starter-alternator for automotive applications. In *Int. Conf. Electrical machines*, pages 1802-1808, Istanbul, Sep. 1998.
- [3] J.R. Hadji-Minaglou and G. Henneberger. Comparison of different motor types for electric vehicle application. *EPE Journal*, 8(3-4):46-55, Sep. 1999.
- [4] G. Friedrich, L. Chédot, and J.M. Biedinger. Comparison of two optimal machine design for integrated starter-generator applications. In *Int. Conf. Electrical machines*, Aug. 2002.
- [5] C. Plasse, M. Chemin, G. Lacamoire, and E. von Westerholt. L'alternateur, du stop & go au groupe motopropulseur hybride. In *Congrès de la Société des Ingénieurs Automobile*, Versailles, Nov. 2001.
- [6] C. Plasse, A. Akemakou, P. Armiroli, and D. Seville. L'alternateur, du stop & go au groupe motopropulseur mild hybride. In *Prop'Elec*, Aix-en-Provence, Mar. 2003.
- [7] B. Sneyers, D.W. Novotny, and T.A. Lipo. Field weakening in buried permanent magnet AC motor drives. *IEEE Trans. Ind. Appl.*, 21:398-407, Mar./Apr. 1985.
- [8] A.M. El-Serafi, A.S. Abdallah, M.K. El-Sherbiny, and E.H. Badawy. Experimental study of the saturation and the cross-magnetizing phenomenon in saturated synchronous machines. *IEEE Trans. Energy Conv.*, 3(4):815-823, Dec. 1988.
- [9] P. Vas. *Vector control of AC machines*. Springer, 1990.
- [10] E. Levi. Saturation modelling in d-q axis models of salient pole synchronous machine. *IEEE Trans. Energy Conv.*, 14(1):44, Mar 1999.
- [11] E.C. Lovelace, T.M. Jahns, and J.H. Lang. Impact of saturation and inverter cost on interior PM synchronous machine drive optimization. *IEEE Trans. Ind. Appl.*, 36(3):681-689, May./Jun. 2000.
- [12] C. Mademlis and V. Agelidis. On considering magnetic saturation with maximum torque per current control in interior permanent magnet synchronous motor drives. *IEEE Trans. Energy Conv.*, 16(3):246-252, Sep. 2001.
- [13] B. Stumberger, G. Stumberger, D. Dolinar, A. Hamler, and M. Trlep. Evaluation of saturation and cross-magnetization effects in interior permanent-magnet synchronous motor. *IEEE Trans. Ind. Appl.*, 39(5):1264-1271, Sep./Oct. 2003.
- [14] S. Morimoto, M. Sanada, and Y. Takeda. Effects and compensation of magnetic saturation in flux-weakening controlled permanent magnet synchronous motor drives. *IEEE Trans. Ind. Appl.*, 30(6):1632-1637, Sep./Oct. 1994.
- [15] S.-A. Tahan and I. Kamwa, "A two-factor saturation model for synchronous machines with multiple rotor circuits," *IEEE Trans. Energy Conv.*, vol. 10, no. 4, pp. 609-616, Dec. 1995.
- [16] L. Chédot and G. Friedrich. Comparison of direct and adaptive optimal controls for interior permanent magnet synchronous integrated starter generator. In *Int. Elec. Mach. Drive Conf.*, Madison, WI, Jun. 2003.
- [17] L. Chédot and G. Friedrich. A cross saturation model for a permanent magnet synchronous machine. Application to a starter-generator. In *IAS annual meeting*, Seattle, Oct. 2004.
- [18] L. Chédot and G. Friedrich. Optimal control of interior permanent magnet synchronous integrated starter-generator. In *Conf. European Power Electronics Ass.*, Toulouse, Sep. 2003.
- [19] S. Morimoto, M. Sanada, and Y. Takeda. Wide-speed operation of interior permanent magnet synchronous motors with high-performance current regulator. *IEEE Trans. Ind. Appl.*, 30(4):920-926, Jul./Aug. 1994.
- [20] C. Lesbroussart. Etude d'une stratégie de modulation de largeur d'impulsions pour un onduleur de tension triphasé à deux ou trois niveaux : la Modulation Delta Sigma Vectorielle. PhD thesis, Université de Technologie de Compiègne, Laboratoire d'Electromécanique de Compiègne, 1997.
- [21] J. Hobraiche. Comparaison de stratégies de modulation de largeur d'impulsions – Application à l'alternateur-démarrateur.

PhD thesis, Université de Technologie de Compiègne, Laboratoire d'Electromécanique de Compiègne, 2005. En cours.

- [22] E. Kuhn. Modèle de batterie NiMH pour véhicule hybride parallèle : validation en grands signaux. In JCGE, Nantes, 2003.
- [23] R.I. Davis and R.D. Lorenz. Engine torque ripple cancellation with an integrated starter alternator in a hybrid electric vehicle: implementation and control. IEEE Trans. Ind. Appl., 39(6):283-296, Nov./Dec. 2003.